Theoretical model for the Frank elastic moduli in the intercalated SmA b phase of bent-shaped dimers

Claire Meyer, Tatiana Sergan, Vassili Sergan, Daniel Stoenescu, Patrick Davidson, Anamarija Knežević, Irena Dokli, Andreja Lesac, Ivan Dozov

Theoretical model for the Frank elastic moduli in the intercalated SmA_b phase of bent-shaped dimers

Claire Meyer[1*], Tatiana Sergan[2], Vassili Sergan[2], Daniel Stoenescu[3], Patrick Davidson[4], Anamarija Knežević[5], Irena Dokli[5], Andreja Lesac[5] and Ivan Dozov[1,4]

[1]Physique des Systèmes Complexes, Université de Picardie Jules Verne, 80039 Amiens, France
[2]California State University, Sacramento, 6000 J Street, Sacramento, California 95608, USA
[3]Optics Department, IMT Atlantique, CS 83818, 29238 Brest cedex, France
[4] Laboratoire de Physique des Solides, Université Paris-Saclay, CNRS, 91405 Orsay, France
[5]Ruđer Bošković Institute, Bijenička 54, 10000 Zagreb, Croatia

In our previous works we have shown that the elastic properties of the intercalated SmA_b phase formed by bent-shaped dimers are governed by the nematic-like behaviour of the secondary director **m** that is associated with the projection of the molecular axes of the monomers on the plane of the smectic layer. From the experiment, the corresponding three Frank-like moduli K_{11}^m, K_{22}^m and K_{33}^m related to the secondary director demonstrate the usual behaviour of the Frank moduli of the nematics formed by rod-like molecules: monotonously increase with decreasing temperature. This is contrary to the temperature dependence of the elastic moduli for the primary director of N and N_{TB} phases formed by bent-shaped dimers (for which the bend elastic constant decreases with temperature to zero). However, the values of the Frank-like moduli for SmA_b were found to be smaller than their nematic-phase equivalents, and demonstrate a strong and unusual anisotropy, with $K_{11}^m : K_{22}^m : K_{33}^m$ ratio being approximately 30 : 1 : 10. Here we present a theoretical model based on the assumption of the nematic-like order within the smectic layers that provides a qualitative explanation of the experimental results.

I. INTRODUCTION

The most commonly used liquid crystals (LCs) are uniaxial anisotropic fluids formed by rod-like molecules oriented with their longest molecular axes along an average direction called the director, which is a unit vector **n** defining the D_∞ symmetry axis of the LC phase. Fluids that have only orientational order but no positional order are called nematics. A distortion of the director field in nematics requires an elastic energy given by [1]:

$$f^n = \frac{1}{2}\left[K_{11}\big(\mathbf{n}(\boldsymbol{\nabla}\cdot\mathbf{n})\big)^2 + K_{22}\big(\mathbf{n}\cdot(\boldsymbol{\nabla}\times\mathbf{n})\big)^2 + K_{33}\big(\mathbf{n}\times(\boldsymbol{\nabla}\times\mathbf{n})\big)^2\right], \quad (1)$$

where the vectors $\mathbf{n}(\boldsymbol{\nabla}\cdot\mathbf{n})$ and $\mathbf{n}\times(\boldsymbol{\nabla}\times\mathbf{n})$ and the pseudo-scalar $\mathbf{n}\cdot(\boldsymbol{\nabla}\times\mathbf{n})$ describe the splay, bend, and twist distortions of the director **n**, respectively, and K_{11}, K_{33}, and K_{22} are the respective elastic moduli.

In an external electric field, the free energy of the LC per unit volume becomes:

$$f^n = \frac{1}{2}\left[K_{11}\big(\mathbf{n}(\boldsymbol{\nabla}\cdot\mathbf{n})\big)^2 + K_{22}\big(\mathbf{n}\cdot(\boldsymbol{\nabla}\times\mathbf{n})\big)^2 + K_{33}\big(\mathbf{n}\times(\boldsymbol{\nabla}\times\mathbf{n})\big)^2 + \boldsymbol{D}\cdot\boldsymbol{E}\right], \quad (2)$$

where $\boldsymbol{E}$ is the external electric field and $\boldsymbol{D}$ is the electric displacement. When a voltage is applied across a uniformly aligned nematic layer, the director field is distorted and the new director configuration results from a balance of elastic and electric torques, the latter arising from the anisotropy of the dielectric permittivity of nematics. This effect, known as the electric Fréedericksz transition (FrTr) [2,3], is used to control the optical properties of the LC sample by an electric field thanks to the optical anisotropy of LCs, a phenomenon exploited for applications in modern displays.

In addition to long-range orientational order, smectic (Sm) phases, unlike nematics, have long-range positional order, with LC molecules arranged in equidistant layers. The simplest of these phases, the smectic A (SmA), is formed by rod-shaped molecules parallel to the normal to the layers. Molecular compounds with more complicated shape, such as bent-shaped dimers, can also form SmA-like phases. However, in this case, their shape imposes additional constraints on the structure of the layers, leading to unusual physical properties of the phase. For example, in previous work [4], we reported a new electro-optic effect in a biaxial smectic A phase (SmA_b) formed by bent-shaped dimers that is similar to the FrTr in nematics. In references [4, 5] we have described the structural, dielectric, optical, and elastic properties of one such system, hereafter referred to as BP12, which is a mixture of a bent-shaped dimer, 1,7-Bis(6-(4-

hexyloxybenzoyloxy)naphthalene-2-yl)heptane (referred to as BNA-76) with the rod-like nematogen 4′-cyano[1,1′-biphenyl]-4-yl 4-hexylbenzoate (6-PEPP-N). The phase transition temperatures of the mixture measured by DSC are: Iso – 162 °C - N - 109 °C - N_{TB} - 102 °C - SmA_b - ~ 70 °C - Cr. (Note that the N_{TB} and the SmA_b phase coexist in a wide temperature range, from 102 to 97 °C.) The elastic properties of the SmA_b phase are the main topic of this article.

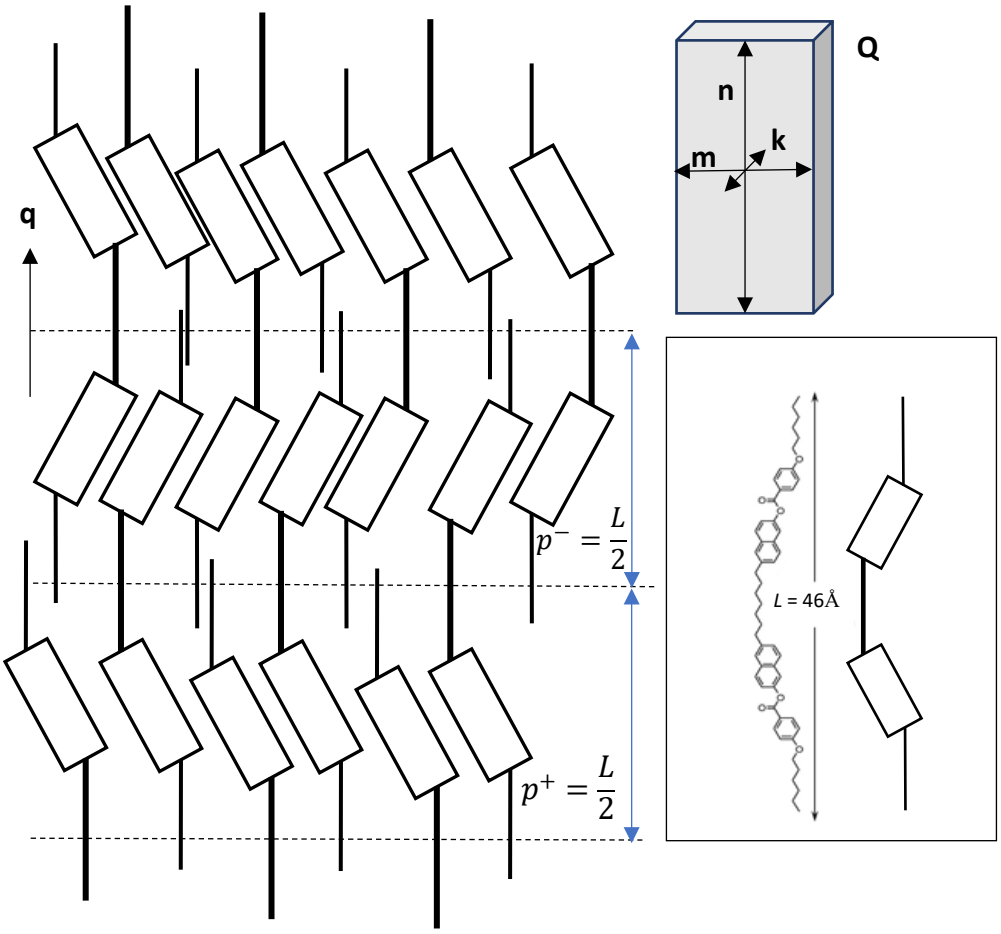

Fig. 1. Schematic representation of the intercalated SmA_b phase. Each dimer spans two adjacent smectic layers, with the tilt angle of the monomer alternating from layer to layer. The orientational order tensor, **Q**, of the dimers (shown in grey) is biaxial. The primary director, **n**, is oriented along the long axis of the dimer and is perpendicular to the smectic layers. The secondary director, **m**, is perpendicular to **n** and lies in the plane of the dimer. The third director, **k**, is perpendicular to both **n** and **m**. The inset shows the molecular structure [4] and a schematic representation of the dimer. The vector **q** is a unit vector perpendicular to the smectic layers.

The SmA_b phase, whose structure is shown in Figure 1, retains all the properties of the ordinary SmA phase. The expression of its elastic energy has, in addition to the terms associated with the distortions of the primary director **n** given by Eq. (1), terms related to the compression and/or dilation of the smectic layers and to the tilt of **n** away from the normal to the layers, **q**. The elastic energy corresponding to these specific smectic terms is much higher than those related to the distortions of **n**. Moreover, due to the incompatibility of the bend and twist distortions of **n** with the layered structure, these modes cannot be observed, and therefore only a splay distortion can take place. Consequently, the ordinary Fréedericksz transition is forbidden because of the prohibitively high energy cost of tilting the primary director **n** away from **q**.

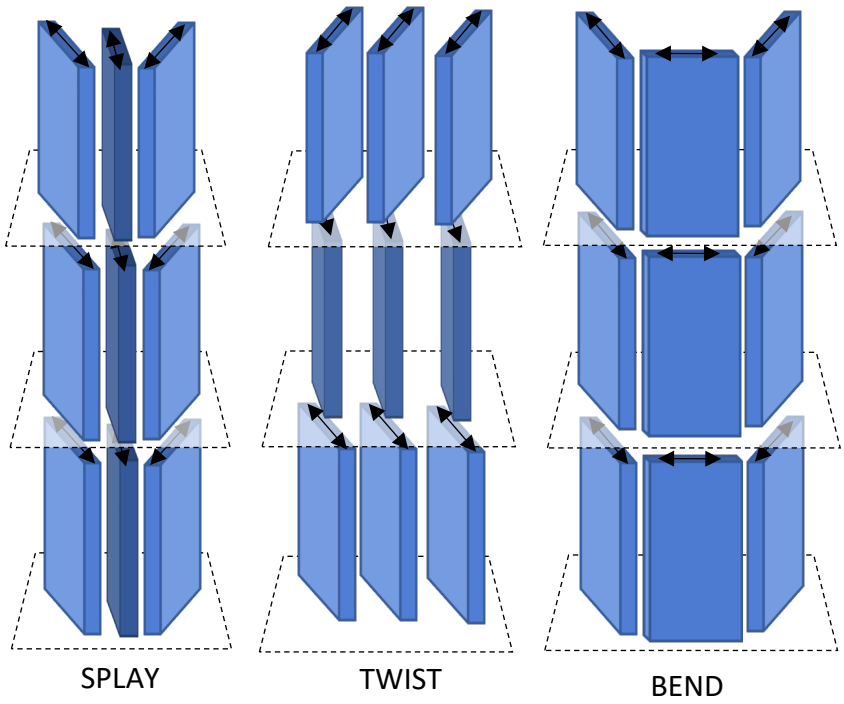

modes of the secondary director **m** (shown as double-headed arrow) in the SmA_b phase The splay and bend distortions are shown within a single layer, the twist distortion spans three adjacent layers. The relative angle between the dimers is greatly exaggerated for clarity.

However, the plank-like shape of the dimer [6, 7, 8] gives the system additional degrees of freedom. Rotation of the dimers about their long axis relative to each other requires little energy, allowing for nematic-like distortions of the secondary director, **m** (see Figure).

Since **m** and **n** are decoupled, the elastic distortion energy of a planar SmA_b sample can be written in a form mathematically identical to that of the regular uniaxial nematic:

$$f^m = 1/2\,\{K_{11}^m\,[\mathbf{m}(\nabla \cdot \mathbf{m})]^2 + K_{22}^m\,[\mathbf{m} \cdot (\nabla \times \mathbf{m})]^2 + K_{33}^m\,[\mathbf{m} \times (\nabla \times \mathbf{m})]^2\}\,. \qquad (3)$$

Here K_{ii}^m, for i = 1, 2, 3, are the elastic moduli for splay, twist, and bend distortions of **m**, respectively [4].

In our previous work [5], we measured the temperature dependence of all three K_{ii}^m for the BP12 mixture using a variety of dielectric, electro-optical, and optical methods. The results (reproduced from Ref. 5 in Fig. 3) were quite surprising: the temperature dependence of K_{11}^m and K_{33}^m in the SmA_b phase is qualitatively similar to that of a regular rod-like nematic, as both constants decrease with increasing temperature and, although slightly smaller, are still of the same order of magnitude as those of 5CB [9]. A striking difference between the usual nematic and the SmA_b is that, for the latter, K_{11}^m is about 3 times larger than K_{33}^m, whereas, for the former, K_{33}^n is similar or slightly larger than K_{11}^n . The property $K_{33}/K_{11} << 1$ is common for bent-shaped dimers when approaching the phase transition to the twist-bend nematic (N_{TB}) phase. In this case, K_{33} even decreases to almost zero on cooling [10]. As for rod-like nematics, the elastic constant K_{33}^m of the SmA_b increases with decreasing temperature (Fig. 3). Note, however, that in the SmA_b phase, K_{11}^m and K_{33}^m are associated with the rotation of the molecules about their long molecular axis, which is less energetically costly than the rotation about the short molecular axis involved in rod-like nematics.

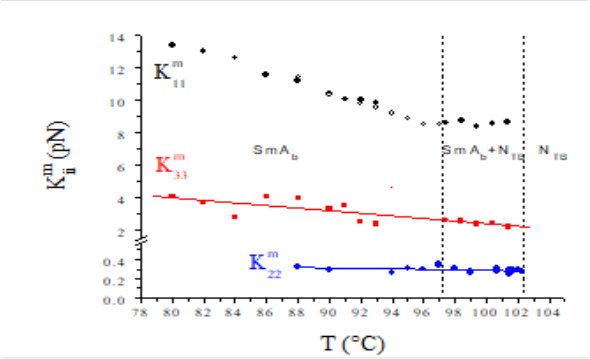

Fig. 3. Temperature dependence of the elastic moduli for the distortions of the **m**-director in the intercalated SmA_b phase of BP12.

Another surprising difference between the SmA_b and usual nematics is that K_{22}^m is ten times smaller than K_{33}^m and about 30 times smaller than K_{11}^m. It is also almost an order of magnitude smaller than K_{22} of the typical 5CB nematic [9]. Qualitatively, this behaviour can be explained by the anticlinic alignment of the monomers in adjacent smectic layers of the intercalated SmA_b phase, which makes the inter-layer nematic-like contribution to K_{22}^m negligible. The residual twist elasticity in the intercalated SmA_b phase should then be attributed to the twist elasticity of the central spacer of the BNA-76 dimers and/or to the decrease of the in-layer order parameter of the monomers within the smectic layer due to the coexistence of two populations of monomers with slightly different orientations of **m**. In this article, we present a theoretical model describing

the mechanism of twist elasticity in the intercalated SmA_b phase. The model explains the unusual behaviour of the K_{ii}^{m} elastic moduli of the SmA_b phase and relates it to the in-plane order of the mesogenic monomers.

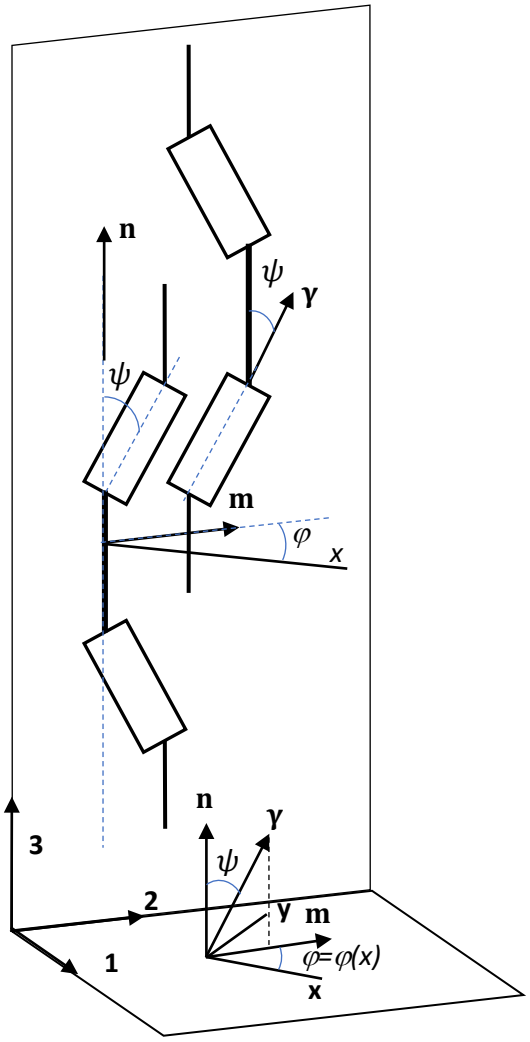

Fig. 4. Coordinate system of the dimers.

II. IN-PLANE ORIENTATIONAL ORDER OF THE MONOMERS

As mentioned above, the long axis of each dimer is perpendicular to the smectic layers (Fig. 1). Moreover, each dimer spans over two adjacent layers, which makes the layers intercalated. In a uniformly oriented SmA_b sample, the planes of the dimers are on average oriented in the same direction as the secondary director **m**. Let's introduce a local Cartesian system of coordinates (**1**, **2**, **3)** associated with a dimer (Fig. 4). In this system, the monomers belonging to the same dimer are in the $\widehat{\mathbf{23}}$ plane, with primary director **n** parallel to the **3**-axis. The plane of the smectic layer is parallel to the $\widehat{\mathbf{12}}$ plane. Within a single smectic layer, the long axes of the monomers are all oriented in the same direction, given by the vector **γ** (director of the layer), which makes an angle ψ with the **3**-axis and therefore with **n**. All three vectors **n**, **m**, and **γ** are coplanar. In Fig. 4, the **x**-axis is a reference axis parallel to the plane of the layer. The orientation of **m** varies within the smectic layer and we call φ the angle between **m** and the **x**-axis.

Within each smectic layer of the SmA_b, the rod-like monomers tend to align parallel to each other, leading to nematic-like order. Therefore, each individual monomer is oriented in the Maier-Saupe mean-field potential of its neighbors [11]:

$$U_1(\beta) = \frac{u_2}{kT}\langle P_2\rangle P_2(\cos\beta), \tag{4}$$

where β is the angle between the long axis of the monomer and the director $\boldsymbol{\gamma}$, $\langle P_2\rangle = \langle P_2(\cos\beta)\rangle$ is the nematic order parameter, and u_2 is the amplitude of the two-particle potential. Moreover, the contribution of the alkyl spacer to the mean-field potential is negligible due to its low anisotropy of polarizability. Thus, the orienting potential acting on each dimer is just twice that acting on each monomer of the dimer.

Here, we consider the monomer layer as a thin slab of nematic formed by free (non-dimerized) monomer moieties with director $\boldsymbol{\gamma}$ tilted at an angle ψ with respect to the normal to the layers. In general, the order parameter of the monomer slab, S_{sl}, should be smaller than that of the bulk nematic, S_b, because the two-particle potential is only integrated over a single layer instead of the whole bulk sample. In the case of anticlinic alignment, the contribution to u_2 due to the interaction of two adjacent layers can be neglected because of their opposite signs of the tilt angle. In fact, the average angle between the monomers belonging to two adjacent layers, 2ψ, is about 60°, which is close to the "magic angle" μ at which $P_2(\cos\mu) = 0$.

As can be seen on Fig. 2, any distortion of $\mathbf{m}$ leads to in-layer or layer-to-layer rotation of $\mathbf{m}$ and $\boldsymbol{\gamma}$. In an aligned sample, with the lowest energy of the ground state, $\mathbf{m}$ is uniform, and its in-plane orientation is arbitrary. In this case, $\boldsymbol{\gamma}$ is in the $\widehat{\mathbf{n},\mathbf{m}}$ plane, and the sign of its tilt alternates from layer to layer. When $\mathbf{m}$ rotates by an angle φ, all its three main distortion modes are involved (Fig. 2), and $\boldsymbol{\gamma}$ rotates on a cone of aperture ψ. The contribution of each distortion mode to the elastic energy is determined by their respective constants K_{ii}^m. However, according to the nematic-like alignment of the monomers within each layer, this distortion can also be described as the nematic-like distortion of $\boldsymbol{\gamma}$, which is characterized by the Frank elastic moduli, κ_{ii}, of the nematic phase formed by the monomers within the slab. Therefore, the moduli K_{ii}^m can be expressed as functions of κ_{ii}, which is the general strategy that we use in the following sections.

III. SPLAY AND BEND ELASTIC MODULI

To compute K_{11}^m and K_{33}^m, the splay and bend elastic constants of the secondary director **m**, it is sufficient to consider the case where the orientation of **m** varies only with respect to the arbitrary reference axis *x*. These two principal distortions, shown in Fig. 2, can be described as a rotation of **m** in the layer plane along the **x**-axis. In the coordinate system (**x**, **y**, **3**), **m** has components $(\cos\varphi, \sin\varphi, 0)$, and the distortion energy density of the SmA_b in terms of $\varphi = \varphi(x)$ is:

$$f^m = \frac{1}{2}\{K_{11}^m\,[\mathbf{m}(\boldsymbol{\nabla}\cdot\mathbf{m})]^2 + K_{33}^m\,[\mathbf{m}\times(\boldsymbol{\nabla}\times\mathbf{m})]^2\} = \frac{1}{2}\{K_{11}^m \sin^2\varphi + K_{33}^m\cos^2\varphi\}\left(\frac{d\varphi}{dx}\right)^2. \quad (5)$$

In this system, **γ** has components $(\sin\psi\cos\varphi, \sin\psi\sin\varphi, \cos\psi)$ and the sign of ψ alternates from layer to layer. The energy density in terms of the director **γ** of the nematic slab is:

$$f^\gamma = \frac{1}{2}\{\kappa_{11}\,[\boldsymbol{\gamma}(\boldsymbol{\nabla}\cdot\boldsymbol{\gamma})]^2 + \kappa_{22}\,[\boldsymbol{\gamma}\cdot(\boldsymbol{\nabla}\times\boldsymbol{\gamma})]^2 + \kappa_{33}\,[\boldsymbol{\gamma}\times(\boldsymbol{\nabla}\times\boldsymbol{\gamma})]^2\} = \frac{1}{2}\{\kappa_{11}\sin^2\psi\sin^2\varphi +$$

$$(\kappa_{22}\cos^2\psi + \kappa_{33}\sin^2\psi)\sin^2\psi\cos^2\varphi\}\left(\frac{d\varphi}{dx}\right)^2 . \quad (6)$$

As expected, f^γ is independent of the sign of ψ. Finally, the comparison of f^m and f^γ gives the nematic-like elastic moduli K_{11}^m and K_{33}^m as functions of the Frank moduli, κ_{ii}, of the equivalent nematic slab:

$$K_{11}^m = \kappa_{11}\sin^2\psi \quad (7)$$

$$K_{33}^m = \kappa_{22}\sin^2\psi\cos^2\psi + \kappa_{33}\sin^4\psi. \quad (8)$$

IV. TWIST ELASTIC CONSTANT

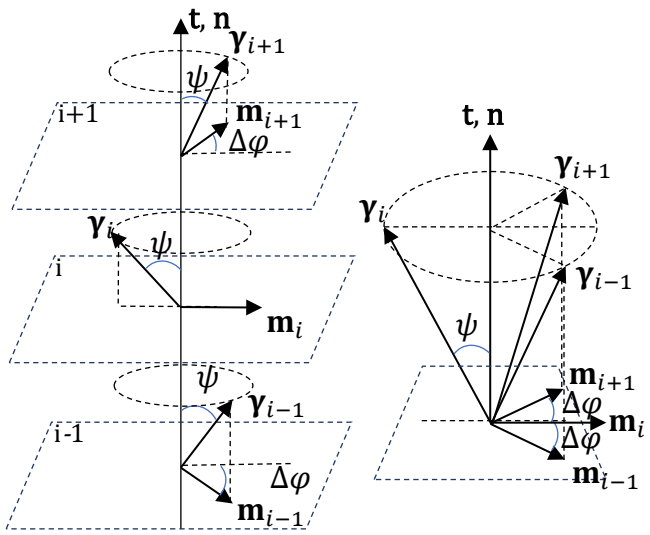

Fig. 5. Geometry of twist deformation of secondary director **m**. Three consecutive smectic layers are shown.

The geometry of a twist distortion of the secondary director, **m**, is more complicated than for splay and bend, because, although **m** is aligned uniformly within each layer, it rotates by a small angle $\Delta\varphi$ from one layer to the next, forming a helix with axis **t** perpendicular to the layers (Fig. 5). The helical pitch is $p_{\mathbf{m}} = \frac{2\pi}{\Delta\varphi} d$, where d is the thickness of the layer of monomers. The **γ** director, in the even /odd layers, rotates on a cone with aperture ψ with an angular step of $\Delta\varphi$. However, due to the anticlinic organisation of the layers, the layer to layer angular step is $\pi - \Delta\varphi$, and corresponding heliconical pitch is $p_{\boldsymbol{\gamma}} = \frac{2\pi}{\pi - \Delta\varphi} d$.

There are three possible contributions for the twist distortion of **m** in an intercalated SmA_b phase. The first results from the twisted nematic-like direct layer to layer interaction. The second is due to the torsional deformation of the alkyl spacer linking two monomers. Such deformation does not alter the relatively high order parameter of the **γ** director within the nematic slab. The third is due to the rotation of the dimer as a whole with respect to other dimers. Unlike usual rod-like molecules, the dimers are plank-shaped, and therefore any rotation of such a plank will disturb the nematic order within the slab and reduce the order parameter of **γ**.

In the following paragraphs we will analyse the relevance of the three mechanisms mentioned above and their contributions to K_{22}^m.

IV.1 CONTRIBUTION OF THE DIRECT INTERACTION BETWEEN ADJACENT MONOMER LAYERS TO K_{22}^m.

The nematic order within the layer *i* favors the orientation of its director $\boldsymbol{\gamma}_i$ parallel to those, $\boldsymbol{\gamma}_{i\pm1}$, of the adjacent layers. The nematic-like energy of interaction between layers *i* and *i*±1 is proportional to $-P_2(\boldsymbol{\gamma}_i \cdot \boldsymbol{\gamma}_{i\pm1})$ [11]. This inter-layer contribution differs greatly between the anticlinic (as in the SmA_b) and synclinic (as in the chiral smectic C, SmC*) organisations of the tilt in adjacent layers. Indeed, as can be seen in Fig. 6a, in a synclinic smectic with tilt ψ and twist $\Delta\varphi$ per layer:

$$\boldsymbol{\gamma}_i = (0, \sin\psi, \cos\psi)$$

$$\boldsymbol{\gamma}_{i+1} = (\sin\psi \sin\Delta\varphi\,,\ \sin\psi\cos\Delta\varphi\,, \cos\psi)$$

in the indicated system of coordinates. Thus,

$$-P_2(\boldsymbol{\gamma}_i \cdot \boldsymbol{\gamma}_{i\pm1}) = -\tfrac{3}{2}(\sin^2\psi\cos\Delta\varphi + \cos^2\psi)^2 + \tfrac{1}{2} \approx -1 + \tfrac{3}{2}\sin^2\psi(\Delta\varphi)^2 \qquad (9)$$

assuming small $\Delta\varphi$ and neglecting terms of higher order in $\Delta\varphi$. The first term here, independent of the twist, is the inter-layer contribution to the self -energy of the phase. It is negative because the directors of the two layers are parallel in the absence of twist. The second term, quadratic in the twist angle per layer, is the inter-layer contribution to the distortion energy. It is proportional to $\sin^2\psi(\Delta\varphi)^2$ and positive because, in the twisted case, the two directors of the adjacent layers are no longer parallel. The contribution of this term to K_{22}^m will be of the order of $\kappa_{22}\sin^2\psi$, assuming that $\kappa_{22} = \kappa_{33}$ for the monomer nematic.

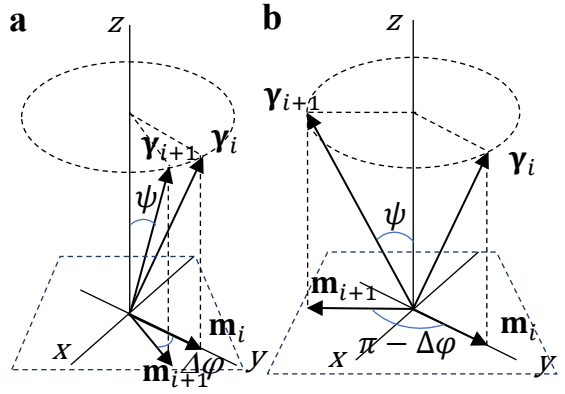

Fig. 6. Schematic representation of the twist in a layered synclinic (a) system with tilt ψ and twist $\Delta\varphi$ per layer and an anticlinic (b) system with the same tilt ψ and twist $\pi - \Delta\varphi$ per layer.

In an anticlinic chiral smectic with tilt ψ and twist $\pi - \Delta\varphi$ per layer (Fig. 6b):

$$\boldsymbol{\gamma}_i = (0, \sin\psi, \cos\psi)$$

$$\boldsymbol{\gamma}_{i+1} = (\sin\psi \sin(\pi - \Delta\varphi)\,, \sin\psi \cos(\pi - \Delta\varphi)\,, \cos\psi) =$$
$$(\sin\psi, \sin\Delta\varphi\,, -\sin\psi\cos\Delta\varphi\,, \cos\psi).$$

Thus, using the same approximations as in the synclinic case, we obtain:

$$(\boldsymbol{\gamma}_i \cdot \boldsymbol{\gamma}_{i\pm1})^2 = (0 - \sin^2\psi\cos\Delta\varphi + \cos^2\psi)^2 = (\cos^2\psi - \sin^2\psi\cos\Delta\varphi - \sin^2\psi + \sin^2\psi)^2 = \left(\cos^2\psi - \sin^2\psi + \sin^2\psi\,(1-\cos\Delta\varphi)\right)^2 = \left(\cos 2\psi + \sin^2\psi\,(1-\cos\Delta\varphi)\right)^2 \approx \left(\cos 2\psi + \frac{1}{2}\sin^2\psi\,(\Delta\varphi)^2\right)^2 \approx \cos^2 2\psi + \cos 2\psi \sin^2\psi\,(\Delta\varphi)^2 \qquad (10)$$

The inter-layer contribution to the energy becomes:

$$-P_2(\boldsymbol{\gamma}_i \cdot \boldsymbol{\gamma}_{i\pm1}) \approx -P_2(\cos 2\psi) - \frac{3}{2}\cos 2\psi \sin^2\psi(\Delta\varphi)^2.$$

The first term, which is twist-independent, again represents the self-energy of the nematic-like order of the phase. Note that, in the anticlinic case, its absolute value decreases with increasing tilt angle and even changes sign when $\cos 2\psi > 1/3$ (i.e. at the magic angle). Here, $\psi \approx 30°$ and $P_2(\cos 2\psi)$ is small and negative, so that the inter-layer contribution to the self-energy can be neglected (see above).

The second term, which is proportional to $(\Delta\varphi)^2$ and represents the contribution of the twist distortion energy to K_{22}^m, also depends on ψ and changes sign at $\psi = 45°$. As in our case $\psi < 45°$, this contribution to the energy is *negative*, i.e. a twisted sample has a slightly lower energy than an untwisted one. This unusual behaviour is easy to understand geometrically from Fig. 6b: for $\Delta\varphi \neq 0$, the angle between the directors of the two adjacent layers *decreases*, leading to a decrease in the interaction energy. Therefore, the contribution of this term to K_{22}^m will be of the order of $-\kappa_{22}\cos 2\psi \sin^2\psi$, assuming again that $\kappa_{22} = \kappa_{33}$ for the monomer nematic. Then, we will neglect this small negative contribution and will focus on other, less direct, contributions to the twist energy of the SmA_b, which are related to its structure made of intercalated dimers.

IV.2 ESTIMATE OF THE CONTRIBUTION OF TWIST DEFORMATION OF THE ALKYL SPACER TO K_{22}^m.

We again consider a periodic structure formed by layers (slabs) with nematic order of the monomers. The slabs are intercalated because each dimer spans two adjacent layers. To create a helical structure only by twisting the alkyl spacer, two monomers of the same dimer belonging to two adjacent layers should form an azimuthal angle, $\Delta\varphi$ Then, if the spacer between the monomers is flexible, the average twist angle per single CH_2-CH_2 bond in the spacer is given by $\alpha = \frac{\Delta\varphi}{N}$, where N is the number of bonds in the spacer (Fig. 7). In this case, only the twist of the chain contributes to the twist distortion of the liquid crystal.

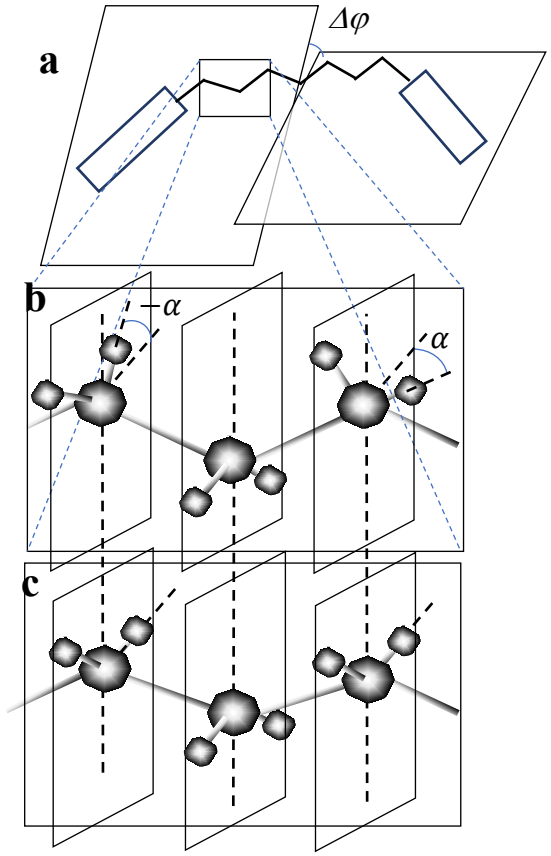

Fig. 7. Schematic representation of the twist of the alkyl spacer between monomers in a dimer molecule. (a) The planes containing the monomers and the normal to the layers form an angle δ, resulting in a layer-to-layer rotation of the **γ**-director. (b) Relative rotation of neighboring CH_2 groups by an angle α (greatly exaggerated for clarity) as compared to an untwisted (all-trans) alkyl chain (c).

The energy needed for twisting a single bond in the spacer by a small angle α is approximately given by [12]:

$$E(\alpha) \approx \Delta E \sin^2\left(\frac{3}{2}\alpha\right) \approx \Delta E \frac{9}{4}\alpha^2. \quad (11)$$

where ΔE is, for example, about 14 kJ/mol for propane [13], and varies slowly with chain length. $E(\alpha)$ has three minima, at $\alpha = 0°$ and $\pm 120°$, with energy barriers in-between (Fig. 8). Thus, if the twist of the spacer is uniformly distributed along its length, then $E(\Delta\varphi) \approx 6E(\alpha) \approx 6E\left(\frac{\Delta\varphi}{6}\right) = \frac{3}{8}\Delta E \Delta\varphi^2$. The energy density (i.e. per unit volume) of the twisted dimers is:

$$f = E(\Delta\varphi)\frac{\rho}{M} \approx 5 \cdot 10^6\ \Delta\varphi^2\ \text{J/m}^3, \quad (12)$$

where $\rho \sim 10^3$ kg/m^3 is the mass density of the SmA_b phase and $M \sim 1$ kg/mol is the molar mass of the dimer. On the other hand, the Frank elastic energy for the same twist is:

$$f_F = \frac{1}{2}K_{22}^m\,[\mathbf{m}\cdot(\boldsymbol{\nabla}\times\mathbf{m})]^2 = \frac{1}{2}K_{22}^m\left(\frac{\Delta\varphi}{d}\right)^2 \approx 10^{17}K_{22}^m\,\Delta\varphi^2 \qquad (13)$$

where d is the thickness of the layer. Here, $d \approx 2.2$ nm, as obtained from the X-ray analysis of the SmA_b structure [4]. Comparing Eq. (10) and (11) provides an estimate of the twist elastic constant of $K_{22}^m \approx 5\cdot 10^{-11}$N, which is more than two orders of magnitude larger than the experimental value of $4\cdot 10^{-13}$N (Fig. 3). This analysis shows that twisting the spacer requires too much energy and therefore does not contribute to the twist distortion of the phase. Consequently, in the following, the dimers will be considered as rigid bodies.

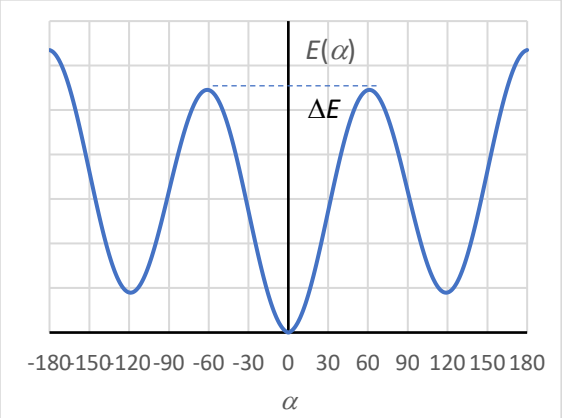

Fig. 8. Simplified $E(\alpha)$ represented according to Eq. (11).

IV.3 ESTIMATE OF THE CONTRIBUTION OF THE ROTATION OF RIGID DIMERS TO K_{22}^m

To estimate the contribution of dimer rotation to K_{22}^m, we consider the twisted SmA_b structure shown in Fig. 9. The director $\mathbf{m}_i$ lies in the plane of the layer and its azimuthal orientation, obtained by averaging the projections of the long molecular axis of the monomers on the plane of the layer, defines the origin of azimuthal angles. Each layer, i, consists of two populations of monomers, belonging to the dimers forming the intercalated layers, characterised by the directors $\mathbf{m}_+$ and $\mathbf{m}_-$ of the dimers, respectively. Within the same layer, i, the directors $\mathbf{m}_+$ and $\mathbf{m}_-$ are rotated by $+\frac{\Delta\varphi}{2}$ and $-\frac{\Delta\varphi}{2}$ with respect to $\mathbf{m}_i$, respectively, and form an angle $\Delta\varphi$. The nematic-like director of the i^{th} layer, $\boldsymbol{\gamma}_i$, lies at the azimuthal angle $\varphi = 0$. In the adjacent layers $i \pm 1$, the directors $\boldsymbol{\gamma}_{i-1}$ and $\boldsymbol{\gamma}_{i+1}$ lie in planes at angles $-\Delta\varphi$ and $+\Delta\varphi$, respectively. For the intercalated dimers with monomers that belong to the same layer, the

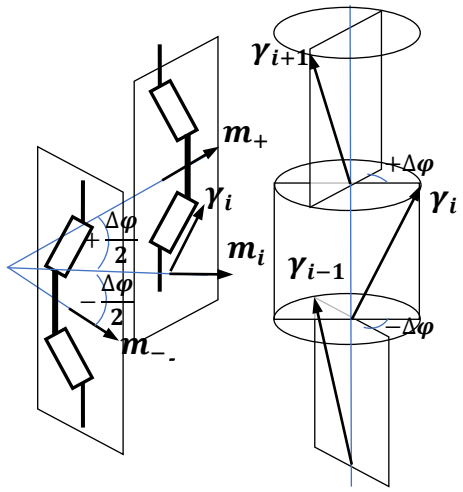

Fig. 9. Schematic representation of the twist in anticlinic SmA_b consisting of rigid dimers.

optimal orientation of the plane of the dimer is at the bisector of the angle between two planes defined by the normal to the layer and $\mathbf{m}_+$ and $\mathbf{m}_-$, respectively (Fig. 9).

In the case of uniform (untwisted) alignment of the SmA_b phase, the nematic order of the monomers in the i^{th} layer is characterised by the director $\boldsymbol{\gamma}_i = (0, \sin\psi, \cos\psi)$. The orientational distribution function (ODF) is:

$$f(\beta) = \frac{1}{2}[1 + 5\langle P_2\rangle P_2(\cos\beta) + 9\langle P_4\rangle P_4(\cos\beta) + \cdots], \quad (14)$$

where β is the angle between the long axis of the monomer and the director $\boldsymbol{\gamma}_i$, $P_l(\cos\beta)$ is the Legendre polynomial, and $\langle P_l\rangle = \langle P_l(\cos\beta)\rangle$ is the order parameter, both of rank l.

In the case of a twist distortion of the SmA_b phase, there are in each layer two distinct populations of monomers. The first population consists of the monomers belonging to the dimers that span the layers i and i +1. The director $\boldsymbol{\gamma}^+$ associated with this population has components $\boldsymbol{\gamma}^+ = (\sin\psi \sin\frac{\varphi}{2}, \sin\psi \cos\frac{\varphi}{2}, \cos\psi)$ and its ODF is given by:

$$f^+(\beta^+) = \frac{1}{2}[1 + 5\langle P_2^+\rangle P_2(\cos\beta^+) + 9\langle P_4^+\rangle P_4(\cos\beta^+) + \cdots]. \quad (15)$$

The second population consists of the monomers belonging to dimers that span over the layer i - 1 and i, and are characterized by the director $\boldsymbol{\gamma}^- = (-\sin\psi \sin\frac{\varphi}{2}, \sin\psi \cos\frac{\varphi}{2}, \cos\psi)$ and ODF:

$$f^-(\beta^-) = \frac{1}{2}[1 + 5\langle P_2^-\rangle P_2(\cos\beta^-) + 9\langle P_4^-\rangle P_4(\cos\beta^-) + \cdots]. \quad (16)$$

(Here $\beta^\pm$ and $\langle P_L^\pm\rangle$ are defined in the same way as in the case of the uniform SmA_b.) In the twisted SmA_b, the total ODF splits into two terms: $f^t(\beta^t) = \frac{1}{2}[f^+(\beta^+) + f^-(\beta^-)]$, which leads to an increase in the free energy of the nematic (Fig.10) and a decrease in the nematic-like order within the layer. This effectively lowers the order parameter within the layer and requires additional condensation energy. To estimate this energy cost we consider the potential energy

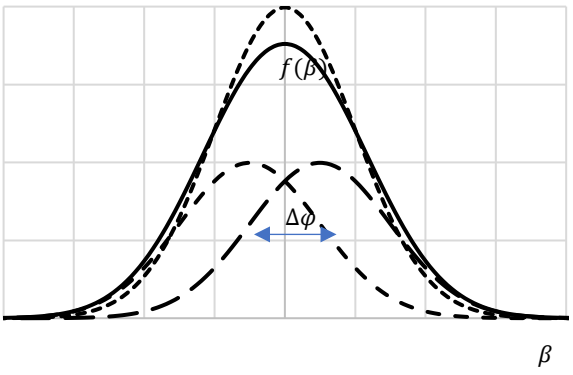

Fig. 10. Schematic 2D presentation of $f^-(\beta^-)$ (long dashes), $f^+(\beta^+)$ (medium dashes), $f^+(\beta^+) + f^-(\beta^-)$ (solid line) and $f(\beta)$ (short dashes). $\Delta\varphi$ is the twist angle per layer.

$U_1(\beta)$ of a single monomer in the mean field of all the others. For $\Delta\varphi = 0$, the Maier-Saupe potential is:

$$U_1(\beta) = u_2\langle P_2(\cos\beta)\rangle P_2(\cos\beta), \qquad (17)$$

where u_2 is the amplitude, in kT units, of the bi-particle potential averaged over all possible values of the radius-vector of the particle separation, β is the angle between the long axis of the monomer, labelled **L**, and the director $\boldsymbol{\gamma}_i$, with $\cos\beta = \mathbf{L}\cdot\boldsymbol{\gamma}_i$. The order parameter of the untwisted state is:

$$S_0 = S(\Delta\varphi = 0\,) = \langle P_2(\cos\beta)\rangle = \int_{-1}^{1} P_2(\cos\beta) f(\beta) d\cos\beta. \qquad (18)$$

In the case of the twisted distortion and due to the splitting of the ODF, the potential is:

$$U_1(\beta) = \frac{1}{2}u_2[\langle P_2(\cos\beta^+)\rangle P_2(\cos\beta^+) + \langle P_2(\cos\beta^-)\rangle P_2(\cos\beta^-)] = \frac{1}{2}u_2 S_0[P_2(\cos\beta^+) + P_2(\cos\beta^-)], \qquad (19)$$

where $\beta^{\pm}$ is defined as above. We assume that the distribution functions of the two populations of monomers are the same as in the untwisted case: $f(\beta) = f^+(\beta^+) = f^-(\beta^-)$.

To facilitate the calculation, we introduce a modified cartesian coordinate system (**1, 2, 3**) with the *2*-axis in the same direction as the *y*-axis in the **L -** centred system and the *3*-axis coinciding with $\boldsymbol{\gamma}_i$ (Fig. 11).

(21)

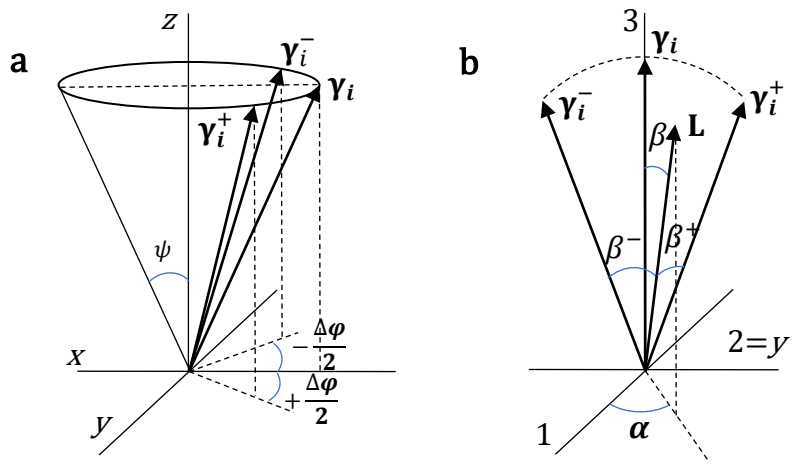

$\boldsymbol{\gamma}_i = (-\sin\psi, 0, \cos\psi)$

$\boldsymbol{\gamma}_i^+ = (-\sin\psi\cos\frac{\Delta\varphi}{2}, \sin\psi\sin\frac{\Delta\varphi}{2}, \cos\psi)$

$\boldsymbol{\gamma}_i^+ = (-\sin\psi\cos\frac{\Delta\varphi}{2}, -\sin\psi\sin\frac{\Delta\varphi}{2}, \cos\psi)$

$\boldsymbol{\gamma}_i = (0, 0, 1)$

$\mathbf{L} = (\sin\beta\cos\alpha, \sin\beta\sin\alpha, \cos\beta$

$\mathbf{L}\cdot\boldsymbol{\gamma}_i = \cos\beta$

Fig. 11. (a) Standard cartesian system of coordinates (**x, y, z**) and (b) modified system of coordinates (**1, 2, 3**). The modified system is obtained by rotating the standard system about the *y*-axis by an angle ψ counter-clockwise. The vectors $\boldsymbol{\gamma}_i$, $\boldsymbol{\gamma}_i^+$,$\boldsymbol{\gamma}_i^-$, **L** and their components in the standard and modified coordinate systems are also shown.

Thus, in the (**1, 2, 3**) system:

$$\boldsymbol{\gamma}_i^+ = \boldsymbol{\gamma}_i^+(\Delta\varphi) = \left(\sin\psi\cos\psi\left(1-\cos\frac{\Delta\varphi}{2}\right), \sin\psi\sin\frac{\Delta\varphi}{2}, 1-\sin^2\psi\left(1-\cos\frac{\Delta\varphi}{2}\right)\right) \approx \left(\frac{1}{8}\sin\psi\cos\psi\Delta\varphi^2, \frac{1}{2}\sin\psi\,\Delta\varphi, 1-\frac{1}{8}\sin^2\psi\,\Delta\varphi^2\right) \quad (20)$$

(Here we kept terms up to $\Delta\varphi^2$).

$$\cos\beta^+ = \mathbf{L}\cdot\boldsymbol{\gamma}_i^+ = \frac{1}{8}\sin\psi\cos\psi\sin\beta\cos\alpha\,\Delta\varphi^2 + \frac{1}{2}\sin\psi\sin\beta\sin\alpha\,\Delta\varphi + \cos\beta - \frac{1}{8}\sin^2\psi\cos\beta\,\Delta\varphi^2 = \cos\beta + A\Delta\varphi + B\Delta\varphi^2, \quad (21)$$

where

$$A = \frac{1}{2}\sin\psi\sin\beta\sin\alpha \quad (22)$$

$$B = \frac{1}{8}(\sin\psi\cos\psi\sin\beta\cos\alpha - \sin^2\psi\cos\beta). \quad (23)$$

Squaring Eq.21 and keeping terms up to $\Delta\varphi^2$ gives:

$$\cos^2\beta^+ \approx \cos^2\beta + 2A\cos\beta\,\Delta\varphi + (A^2 + 2B\cos\beta)\Delta\varphi^2. \quad (24)$$

Since $\boldsymbol{\gamma}_i^+(-\Delta\varphi) = \boldsymbol{\gamma}_i^-(\Delta\varphi)$:

$$\cos^2\beta^- \approx \cos^2\beta - 2A\cos\beta\,\Delta\varphi + (A^2 + 2B\cos\beta)\Delta\varphi^2. \quad (25)$$

Combining equations (24) and (25) and introducing the Legendre polynomials $P_2(\cos\beta^\pm) = \frac{1}{2}(3\cos^2\beta^\pm - 1)$ and $P_2(\cos\beta) = \frac{1}{2}(3\cos^2\beta - 1)$ one obtains:

$$\frac{1}{2}\left(P_2(\cos\beta^+) + P_2(\cos\beta^-)\right) = \frac{3}{4}(\cos^2\beta^+ + \cos^2\beta^-) - \frac{1}{2} = \frac{3}{2}\cos^2\beta - \frac{1}{2} + (A^2 + 2B\cos\beta)\Delta\varphi^2 = P_2(\cos\beta) + \frac{1}{4}(\sin^2\psi\sin^2\beta\sin^2\alpha + \sin\psi\cos\psi\sin\beta\cos\beta\cos\alpha - \sin^2\psi\cos^2\beta)\,\Delta\varphi^2. \quad (26)$$

This expression is biaxial due to the α-dependence in the last term. Averaging over α results in:

$$\frac{1}{2\pi}\int_0^{2\pi}\frac{1}{2}\left(P_2(\cos\beta^+) + P_2(\cos\beta^-)\right)d\varphi = P_2(\cos\beta) + \frac{1}{4}\sin^2\psi\left(\frac{1}{2}\sin^2\beta - \cos^2\beta\right)\Delta\varphi^2 = P_2(\cos\beta)\left(1 - \frac{1}{4}\sin^2\psi\,\Delta\varphi^2\right). \quad (27)$$

Finally, the one-particle potential is now:

$$U_1(\beta) = u_2\left(1 - \frac{1}{4}\sin^2\psi\,\Delta\varphi^2\right)S_0P_2(\cos\beta). \quad (28)$$

This expression is different from the usual Maier-Saupe form, however, renormalization of the order parameter in terms of the per-layer twist angle $\Delta\varphi$ results in

$$\langle P_2(\cos\beta)\rangle = S(\Delta\varphi) = S_0\left(1 - \frac{1}{4}\sin^2\psi\,\Delta\varphi^2\right) = S_0 - \delta S,$$

where $\delta S = S_0\frac{1}{4}\sin^2\psi\,\Delta\varphi^2$ and brings (28) to a more familiar form:

$$U_1(\beta) = u_2S(\Delta\varphi)P_2(\cos\beta). \quad (29)$$

Thus, the standard Maier-Saupe model is applicable:

$$f(\beta) = \frac{1}{Z}e^{\frac{-U_1(\beta)}{kT}} \text{ with } Z = \int_{-1}^{1}e^{\frac{-U_1(\beta)}{kT}}d\cos\beta \text{ and } S = \langle P_2(\cos\beta)\rangle = \int_{-1}^{1}P_2(\cos\beta)\ f(\beta)d\cos\beta. \quad (30)$$

As a next step, we calculate the free energy of the twisted state. The molar free energy in SI units is [14]:

$$A_m = -\frac{1}{2}N_Au_2S^2 - RT\ln Z = \left(-\frac{1}{2}\frac{u_2}{kT}S^2 - \ln Z\right)RT. \quad (31)$$

Correspondingly, the free energy density is $A_V = A_m\frac{\rho}{M}$, where [4] $\rho \approx 10^3$ kg/m^3 is the density of the substance, $M \approx$ 0.4 kg/mol is the molar mass of the monomer, $T \approx$ 400K (which is close to the experimental conditions), and $R = 8.314$ J/(mol·K) is the universal gas constant. Thus,

$A_V = \frac{\rho}{M} RTE(S) \approx 2500\, A_m \approx 8 \cdot 10^6 E(S)$, where $E(S) = -\frac{1}{2}\frac{u_2}{kT} S^2 - \ln Z$.

Then, we have for the untwisted and twisted cases:

$$A_V|_{S_0} = A_V|_{\Delta\varphi=0} = \frac{\rho}{M} RTE(S_0) \tag{32}$$

$$A_V|_S = A_V|_{S_0-\delta S} = \frac{\rho}{M} RTE(S_0 - \delta S) \tag{33}$$

and therefore the variation in free energy density is:

$$\delta A_V = A_V|_S - A_V|_{S_0} = \frac{\rho}{M} RT \frac{dE}{dS}|_{S=S_0}(-\delta S) = \frac{\rho}{M} RT \frac{dE}{dS}|_{S=S_0} \left(-\frac{1}{4} S_0 \sin^2\psi\, \Delta\varphi^2\right) \tag{34}$$

This variation corresponds to an increase in the condensation energy density of the "monomer nematic" and is equivalent to the twist distortion energy density of the SmA_b:

$$\delta A_V = \frac{1}{2} K_{22}^m \left(\frac{\Delta\varphi}{d}\right)^2. \tag{35}$$

Comparison of equations (34) and (35) then gives:

$$K_{22}^m = -\frac{1}{4} S_0 \sin^2\psi\, d^2 \frac{\rho}{M} RT \frac{dE}{dS}|_{S=S_0}. \tag{36}$$

Eq. (36) is then used to calculate K_{22}^m.

IV.4 NUMERICAL CALCULATIONS OF K_{22}^m

We calculate $S_0 = S_0(-\frac{u_2}{kT})$ and $S_0 \frac{dE}{dS}|_{S=S_0}$ numerically, using $-\frac{u_2}{kT}$ as an independent variable. In our calculations we keep $-\frac{u_2}{kT} > \sim 4.5$, which is typical for the nematic phase. K_{22}^m is then calculated according to (36), using $d = 2.2$ nm and $\psi = 30°$ obtained in our previous work [4]. The calculated values of $S_0 \frac{dE}{dS}|_{S=S_0}$ and K_{22}^m are presented in figure 12, along with the measured value of $K_{22}^m = 0.3$ pN (see figure 3), the value of $S_0 = 0.465$ which corresponds to the calculated value (solid line) of $K_{22}^m = 0.3$ pN, and the calculated value of $S_0 \frac{dE}{dS}|_{S=S_0} = -0.075$ at $S_0 = 0.465$. Thus, based on the

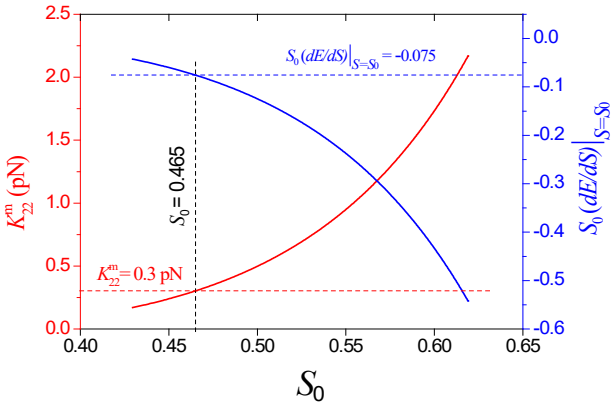

Fig. 12. Calculated $S_0 \frac{dE}{dS}|_{S=S_0}$ (blue line) and K_{22}^m (red line).

measurement of K_{22}^m = 0.3 pN, the results of the model are: $\frac{u_2}{kT}$ = -4.59, S_0 = 0.465, and $S_0 \frac{dE}{dS}|_{S=S_0}$ = -0.075.

V. DISCUSSION.

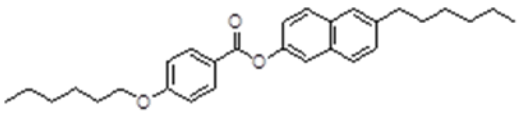

Fig. 13 Chemical structure of BNAM-66

To test the model, we now compare it with the experimental data [4,5]. We have shown that the nematic-like elastic moduli of the SmA_b phase, K_{11}^m and K_{33}^m, can be expressed in terms of the Frank moduli κ_{11}, κ_{22}, and κ_{33} of the equivalent nematic slab and the average tilt angle, ψ, of the monomers in the slab [Eq. (7) and (8)]. Because the monomers forming the dimers have a typical rod-like mesogenic shape, we could measure the elastic properties of a nematogenic compound with chemical structure close to that of the monomer units of the dimers, and then use these measurements to obtain K_{11}^m and K_{33}^m. For this purpose, we synthesised the compound 6-Hexylnaphthalen-2-yl 4-(hexyloxy)benzoate (BNAM-66) (Supporting information) which is very similar to the monomer unit of BNA-76 (Fig. 13). As expected, this compound forms a nematic phase in the temperature range between 84° C and 118 °C. We measured the temperature dependence of all three elastic moduli $\widetilde{K}_{ii}$ of this compound in the nematic phase (the detailed results will be published elsewhere) and found that the $\widetilde{K}_{ii}$ show the behaviour typical of rod-like nematogens: $\widetilde{K}_{33}$ increases from 4.5 pN to 16 pN with decreasing temperature and the ratios of the moduli are temperature independent, with $\widetilde{K}_{33}/\widetilde{K}_{22} \approx 2.5$ and $\widetilde{K}_{33}/\widetilde{K}_{11} \approx 1.1$. After a renormalization procedure taking into account the low order parameter of the equivalent in-layer nematic, the values obtained $\widetilde{K}_{ii}$ were used in Eqs. (7) and (8) to calculate K_{11}^m and K_{33}^m. Using Eqs. (7) and (8) and $\psi \approx 30°$ [4], the estimates $K_{11}^m \approx \frac{1}{4}\kappa_{11}$, $K_{33}^m \approx 0.19\kappa_{22} + \frac{1}{16}\kappa_{33}$, and $K_{33}^m \approx 0.14\kappa_{33} \approx 0.6\, K_{11}^m$ were obtained. Therefore, $K_{33}^m \ll \kappa_{33}$, $K_{33}^m < K_{11}^m$, and $K_{11}^m \ll \kappa_{11}$, which is in good qualitative agreement with the experimental data [4], and, as expected, K_{11}^m/K_{33}^m is essentially independent of temperature. However, more quantitatively, the predicted ratio K_{11}^m/K_{33}^m is lower than the experimentally observed value of ≈ 3.

Our model suggests that the mechanism of twist deformation in the SmA_b phase is quite different from the usual one. The main contribution to the distortion energy comes from a decrease in the condensation energy of the monomer nematic, which effectively lowers the order parameter within the monomer layer. This explains the significant decrease of the twist modulus with respect to the bend modulus in the SmA_b phase. Indeed, the measured value of $K_{22}^m/K_{33}^m \approx 0.1$ is much smaller than the typical one for rod-shaped nematics ($\frac{K_{22}}{K_{33}} \approx 0.3-0.5$), including the BNAM-66 compound. The order parameter for the in-layer orientational order of the monomers estimated from the measured K_{22}^m value is quite low: $S_0 = 0.465$. However, it is still above the threshold value, $S_0 = 0.43$, predicted by the Maier-Saupe model at the nematic-isotropic phase transition.

Our model provides a good qualitative explanation of the unusual behaviour of the nematic elastic moduli K_{ii}^m observed in the SmA_b phase, which includes: (i) a ratio of K_{11}^m to K_{33}^m larger than 1 and independent of temperature; (ii) rather small (compared to usual nematics) values of K_{11}^m and K_{33}^m; (iii) a very small twist elastic modulus K_{22}^m, which is at least an order of magnitude smaller than the same constant for rod-shaped nematics. Quantitatively, however, the measured ratio $K_{11}^m/K_{33}^m \approx 3$ is slightly larger than the value (1.7) predicted by the model. Also, the comparison of the theoretical expressions for K_{11}^m and K_{33}^m with the experimental values suggests that the κ_{11} and κ_{33} moduli of the equivalent in-layer nematic are large, and more strongly temperature dependent. This should reflect the behaviour of the order parameter of the equivalent nematic, S_0, which contradicts the small value and weak temperature dependence of S_0 predicted by the model.

This quantitative discrepancy between model and experiment is likely due to the nature of the mean-field theory used, which requires numerous approximations. The most important approximation is that the equivalent nematic is considered here to be uniaxial. In the SmA_b phase, the molecules of the dimer are oriented normal to the smectic layer and their orientational order parameter is probably large. Due to the rather rigid spacer of the dimer, the zenithal (out-of-layer) average deviation of the monomer axis from the $\boldsymbol{\gamma}$ -director should be much smaller than the azimuthal (in-layer) one. Therefore, the nematic slabs representing the layers of monomers should be biaxial. However, for simplicity, we neglected this biaxiality and treated the equivalent nematic according to the Maier-Saupe model, originally developed for rod-like

nematics. More quantitative agreement can be expected by modelling the equivalent nematic as biaxial rather than uniaxial, but such a model is beyond the scope of the present work.

Several other approximations may also affect the results. For example, we neglected the contribution of the spacer to molecular interactions, which can affect the average molecular tilt angle ψ in the slabs. We also used BNAM-66 as a substitute for the monomer moiety. Moreover, our numerical calculation of the twist elastic modulus K_{22}^m as a function of the order parameter S_0, did not take into account the anticlinic organisation of the monomer layers. If considered, it could increase the estimated value of S_0 and lead to a stronger temperature dependence of the order parameter, which may result in a better agreement with the experimental data.

VI CONCLUSIONS

We have presented a simple model that qualitatively explains the mechanism of nematic-like elasticity associated with distortions of the secondary director **m** in the intercalated biaxial SmA_b phase by a variation of the in-plane orientational order of the monomers. The model qualitatively describes the main properties of the three nematic-like elastic moduli K_{ii}^m, which are: $K_{11}^m/K_{33}^m > 1$, $K_{ii}^m < K_{ii}^n$, $K_{22}^m \ll K_{11}^m, K_{33}^m$, and the independence of the K_{11}^m/K_{33}^m ratio from temperature. Quantitatively, the model gives $K_{11}^m/K_{33}^m \approx 1.7$, which is slightly lower than the experimental value of $K_{11}^m/K_{33}^m \approx 3$. This discrepancy may be the result of the numerous approximations involved in the model that ignores direct layer-to-layer interaction, and/or the use of estimated values of elastic constants.

ACKNOWLEDGEMENTS

This research was supported by the Hu Foundation, California State University, Sacramento; by the Croatian Science Foundation (Grant No. IP-2019-04-7978); by the French-Croatian bilateral program COGITO; by the Agence Nationale pour la Recherche ANR (France) through

Grant BESTNEMATICS, No. ANR-15-CE24-0012; and by the Université de Picardie Jules Verne, Amiens, France.

REFERENCES

1. Frank FC. I. Liquid crystals. On the theory of liquid crystals. Faraday Discuss. 1958;25(0):19-28.
2. Fréedericksz V, Zolina V. Forces causing the orientation of an anisotropic liquid. Trans Faraday Soc. 1933;29:919-930.
3. de Gennes PG, Prost J. The Physics of Liquid Crystals: Clarendon, Oxford; 1994.
4. Meyer C, Davidson P, Constantin D, Sergan V, Stoenescu D, Knezevic A, Dokli I, Lesac A, Dozov I. Freedericksz-Like Transition in a Biaxial Smectic-A Phase. Phys Rev X. 2021;11(3):031012.
5. Meyer C, Davidson P, Sergan T, Sergan V, Stoenescu D, Knezevic A, Dokli I, Lesac A, Dozov I. Nematic-like elastic coefficients of the SmA_b phase. Liquid Crystals. 2023;50(1);157-173.
6. Mandle RJ, Goodby JW. A twist-bend nematic to an intercalated, anticlinic, biaxial phase transition in liquid crystal bimesogens. Soft Matter. 2016;12(5):1436-1443.
7. Hegmann T, Kain J, Diele S, Pelzl G, Tschierske C. Evidence for the existence of the McMillan phase in a binary system of a metallomesogen and 2,4,7-trinitrofluorenone. Angew Chem Int. 2001;40(5):887-890.
8. Eremin A, Diele S, Pelzl G, Nadasi H, Weissflog W, Salfetnikova J, Kresse H. Experimental evidence for an achiral orthogonal biaxial smectic phase without in-plane order exhibiting antiferroelectric switching behavior. Phys Rev E. 2001;64(5):051707.
9. Karat PP, Madhusudana NV. Elastic and Optical Properties of Some 4′-n-Alkyl-4-Cyanobiphenyls. MCLC. 1976; 36(1-2): 51-64.
10. Adlem K, Copic M, Luckhurst G R, Mertelj Parri AO, Richardson RM, Snow BD, Timimi BA, Tuffin RP, Wilkes D. Chemically induced twist-bend nematic liquid crystals, liquid crystal dimers, and negative elastic constants. Phys. Rev. E. 2013; 88: 022503.
11. G. Barbero, L.R.Evangelista Adsorbtion phenomena and Anchoring Energy in Nematic Liquid Crystals Taylor & Francis Group, 2006.
12. Weinhold F. A new twist on molecular shape. Nature. 2001; 411; 539-541.
13. Clayden J, Greeves N, Warren S. Organic chemistry: Oxford University Press; 2001.
14. Humphries RL, James PG, Luckhurst. GR. Molecular field treatment of nematic liquid-crystals. Journal of the Chemical Society-Faraday Transactions 2. 1972;68(6):1031-1044.